Cement and Concrete Research 38 (2008) 1098–1105

Contents lists available at ScienceDirect

Cement and Concrete Research

journal homepage: http://ees.elsevier.com/CEMCON/default.asp

The influence of longitudinal cracks on the corrosion protection afforded reinforcing steel in high performance concrete

Amir Poursaee [a], Carolyn M. Hansson [b,*]

[a] Department of Civil Engineering, Purdue University, West Lafayette, IN, USA
[b] Department of Mechanical Engineering, University of Waterloo, Waterloo, ON, Canada

ARTICLE INFO

Article history:
Received 28 June 2007
Accepted 25 March 2008

Keywords:
Corrosion (C)
High performance concrete (E)
Curing (A)
Crack

ABSTRACT

It is almost impossible to produce crack-free concrete and, therefore, codes of concrete structural design (such as ACI 318 [ACI 318, Building Code Requirements for Structural Concrete, American Concrete Institute: Farmington Hills, MI, USA]) take cracking into account and relate permissible crack widths to exposure conditions. Chloride ingress is significantly enhanced by cracks because the ions can penetrate the concrete cover from the walls of the crack as well as from the outer surface of the concrete [P. P. Win, M. Watanabe, and A. Machida, Penetration profile of chloride ion in cracked reinforced concrete. Cement and Concrete Research, 2004. 34(7): p. 1073–1079]. Thus, while the chlorides reach the steel very rapidly directly through the crack, they also reach adjacent areas of steel more rapidly than in uncracked concrete.

The objective of the project was to ascertain whether high performance concrete (HPC) could provide superior protection to Ordinary Portland Cement Concrete (OPCC) even when the structure was cracked parallel to the reinforcing bars (longitudinal cracks) while being exposed to a de-icing salt environment. Two HPCs, as specified by the Ministry of Transportation of Ontario (MTO) [MTO, SSP 904 S13 High Performance Concrete, Amendment to OPSS 904 Construction Specification for Concrete Structures. 1995, Ontario Provincial Standard Specification] were tested: both used blended silica fume cement (Canadian Type 10 E-SF) and had 25% replacement of the cement by either fly ash or ground granulated blast furnace slag. A Class C-2 ordinary Portland cement concrete was used as control.

In the case of cracks parallel to the rebar, HPC does not appear to have any beneficial influence on the corrosion of bars, which is not surprising in view of the fact that the whole length of the bar is directly exposed to the environment via the crack. In contrast, HPC has been found to provide better protection for steel exposed to transverse cracks than does OPCC. However, the benefits of HPC are not as great as they are for sound (uncracked) concrete. The reasons for the better protection are (i) the greater resistance of HPC to chloride penetration from the walls of the crack, (ii) its greater tendency to crack healing and (ii) the different crack path in HPC.

1. Introduction

Porosity and cracks are the main factors that affect concrete quality from the point of view of protecting reinforcing steel from corrosive species [1–4]. These factors can be controlled by three major parameters: (i) a low water to binder ratio (w/b); (ii) the inclusion of supplementary cementing materials, both of which reduce the porosity and (iii) adequate curing, which will minimise any cracking [5–7]. The term "high performance concrete" can generally be defined as concrete which meets special performance and uniformity requirements that cannot normally be achieved by using conventional materials and normal mixing, placing, and curing practices. However, as in the present study, it is often used to describe a concrete incorporating these parameters, thereby, providing high strength and low permeability.

There are large numbers of studies of chloride penetration rates in HPC (e. g. [8–11]) and some research has been carried out on the rebar corrosion process (e. g. [12–14]) in HPC. These studies show that steel in well compacted and cured reinforced HPC exhibits significantly longer corrosion initiation times [15,16] and lower corrosion rates [17] than those observed in conventional reinforced OPC concretes. This is attributed to the very low level of interconnected porosity in HPC concretes.

While interconnected capillary porosity provides a tortuous path for the ingress of chloride ions, oxygen and moisture into concrete, cracks render a more direct path. The sources of cracks in concrete include shrinkage [18], chemical reactions (e.g. alkali aggregate reaction, [16]), weathering processes (e.g. freezing and thawing [19]), reinforcement corrosion [20] and mechanical loading [21]. Despite the prevalence of cracks in structural concrete, there have

* Corresponding author.
E-mail address: chansson@uwaterloo.ca (C.M. Hansson).

0008-8846/$ – see front matter.
doi:10.1016/j.cemconres.2008.03.018

Table 1
Concrete mixture proportions for making 1 m^3 concrete

Component	OPC	HPC-slag	HPC-fly ash
Type 10 Portland, kg	355	–	–
Type 10SF Portland, kg	–	337	337
Slag, kg	–	113	–
Fly ash, kg	–	–	113
Sand, kg	770	718	718
Stone 20 mm, kg	1070	1065	1065
Water, l	153	158	158
Eucon MRC air entrainment	40 ml/100 kg cementitious	65 ml/100 kg cementitious	65 ml/100 kg cementitious
Water reducer	250 ml/100 kg cementitious	250 ml/100 kg cementitious	250 ml/100 kg cementitious
Superplasticizer	–	2l+1.5l	3l+0.5l
W/CM ratio	0.43	0.35	0.35

been relatively few studies concerning the critical crack widths and other aspects of the effect of cracking on corrosion of rebar in OPC concretes [20–26], and even fewer on the influence of cracking on rebar corrosion in HPC [27–31]. Moreover, all this work has concerned cracks formed transverse to the reinforcing bar.

While there has been some investigation of longitudinal cracks in cover concrete formed as a result of corrosion [32–34], as far as the present authors have been able to ascertain, there is nothing in the literature about the effect of longitudinal structural cracks on the corrosion of the embedded steel in concrete. Such cracks are observed in practice in the concrete structures such as continuously reinforced concrete pavements (CRCP) due to loading or thermal shock, steel reinforced concrete pipes and parking garage slabs, [35–39].

In this paper, the corrosion behaviour of steel bar in longitudinally cracked HPC and OPCC with crack widths <0.3 mm (the MTO's maximum allowable limit) is evaluated and the results are compared with those obtained in sound (i.e. uncracked) concrete and transversely cracked (cracks perpendicular to the rebar) concretes.

2. Experimental procedure

This study involves three different concrete mixtures: one OPCC and two HPCs designed to meet the specifications of the MTO, which require the use of silica fume cement and permit up to 25% cement replacement by either blast furnace slag or class C fly ash [3]. The concretes were provided by Dufferin Concrete and their mixture proportions are given in Table 1.

Three sets of concrete prism samples with embedded plain carbon steel rebar were prepared as follows:

i) with cracks parallel to, and immediately above, the rebar and referred to as "longitudinal cracks";
ii) with cracks perpendicular to the rebar and referred to as "transverse cracks";
iii) without any macrocracks, referred to as "sound concrete".

2.1. Prisms with longitudinal crack

Since it is not practical to evaluate the corrosion behaviour of steel in concrete by gravimetric methods, the rates are usually estimated using electrochemical techniques [40]. The reason for using the term

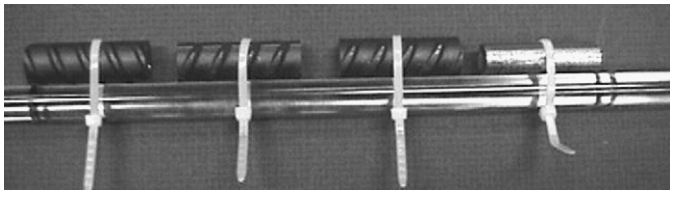

Fig. 1. Corrosion probes showing three black steel elements and one stainless steel element.

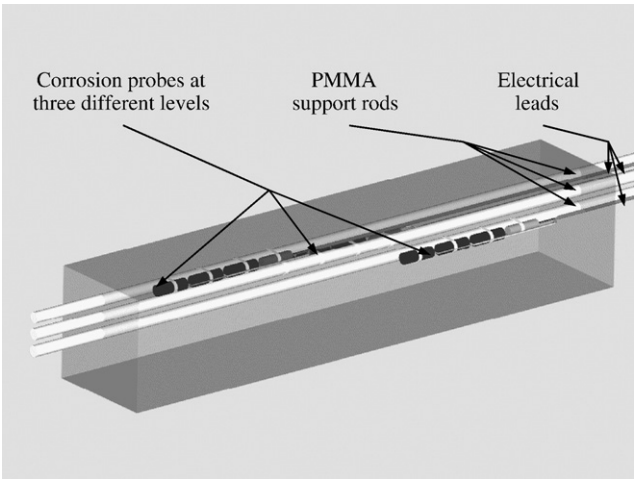

Fig. 2. Schematic illustration of a prism with longitudinal crack. Corrosion probes are embedded in three levels.

"estimate" rather than "determine" is that it is impossible to non-destructively determine the area of steel which is actually undergoing active corrosion without removing the concrete cover. There have been many attempts to design equipment which can limit the area being polarised and, thus, limit the uncertainty in the measurements but these have not been entirely satisfactory [41]. An alternative approach is to limit the actual area of steel by measuring the corrosion on small sections of reinforcing steel (corrosion probes) rather than on the main rebar [42]. The advantage of the embedded probes is knowledge of the maximum area of steel, which could be corroding. The major disadvantages are (i) the limited area for corrosion to initiate; and (ii) the limited area of steel available for the cathodic reduction of oxygen.

Three concrete prisms, 100×100×500 mm, were cast for each of the three concretes. The individual probe elements (30 mm lengths of 10 M bar) were assembled as illustrated in Fig. 1 by attaching them to a polymethylmethacrylate (PMMA) rod, together with a 30 mm length of 316 stainless steel bar as a "reference electrode". All probe elements and the stainless steel were electrically isolated from each other. Probes assemblies were placed at three cover depths, 10 mm and 15 mm, as illustrated schematically in Fig. 2. Casting was carried out indoors in February and the prisms were wet cured according to MTO specification (2 days for OPCC and 7 days for HPCs). After 25 days, the prisms were exposed to the outdoor environment for the remaining period of the project and were covered with a layer of rock salt and kept wet by spraying salt water during the winter months. The composition of the rock salt is given in Table 2.

The outdoor temperature during the experiment was monitored and is shown in Fig. 3. The temperature fluctuations and the difference between thermal expansion coefficient of the PMMA plastic bars ($\sim 75\times10^{-6}$ °C^{-1}) [43] and that of the cement paste, ($\sim 15\times10^{-6}$ °C^{-1}) caused cracking of the concrete parallel to the PMMA bars and, thus, parallel to the rebar probes within the first month of exposure. The cracks were approximately 0.1 mm wide at the surface, as shown in Fig. 4.

The corrosion potential was measured after 128 weeks of exposure and the corrosion rates were determined using the potentiostatic Linear Polarisation Resistance (LPR) technique after 35 weeks and 128 weeks exposure.

Table 2
Relative proportions of ions in rock salt

Cation	% by weight	Anion	% by weight
Ca^{2+}	18.7×10^{-4}	Cl^-	58.83
K^+	2.4×10^{-4}	NO_3^{2-}	1.5×10^{-4}
Mg^{2+}	1.5×10^{-4}	SO_4^{2-}	38.9×10^{-4}
Na^+	40.5		

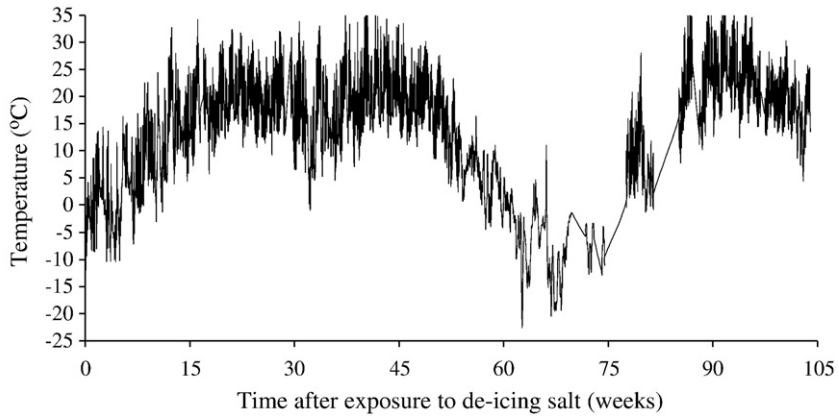

Fig. 3. Outdoor temperature variations during the experiment on the samples with longitudinal cracks.

Fig. 4. 0.1 mm longitudinal crack, caused by thermal expansion coefficient difference between PMMA and concrete.

2.2. Prisms with transverse crack

As reported in detail elsewhere [44], prisms of dimension 100×100×500 mm with rebar probes were cast from each of the three concretes. The cover to the probes was 45 mm. The corrosion probes, similar to those in the prisms with longitudinal cracks but with five black steel segments and one stainless steel segment, were used and were attached to a black steel rebar (instead of PMMA) with a slight overlap to

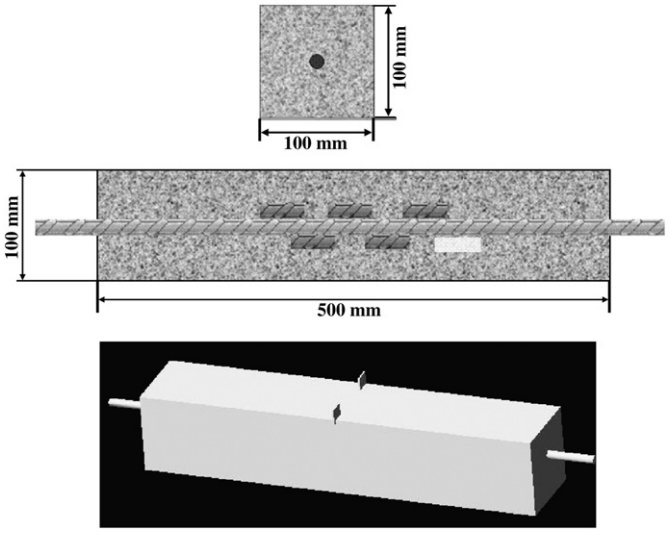

Fig. 5. Schematic plan of the a prism with 0.1 mm induced transverse crack.

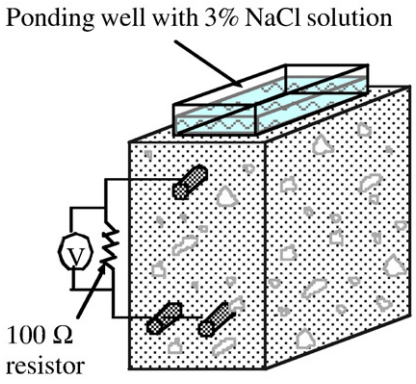

Fig. 6. ASTM G-109 specimen.

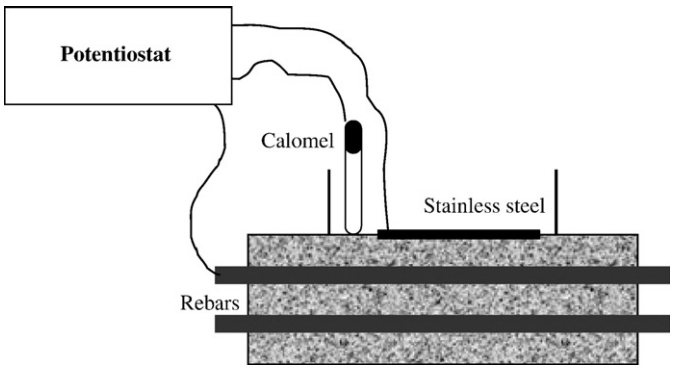

Fig. 7. Schematic plan of the LPR measurement setup on G109 specimens.

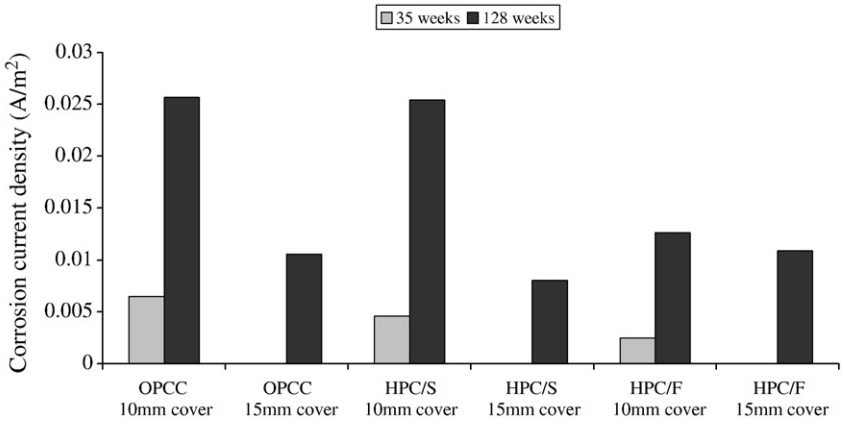

Fig. 8. Corrosion current density of the probes in prisms with 0.1 mm longitudinal crack, 35 and 128 weeks after exposure to de-icing salt.

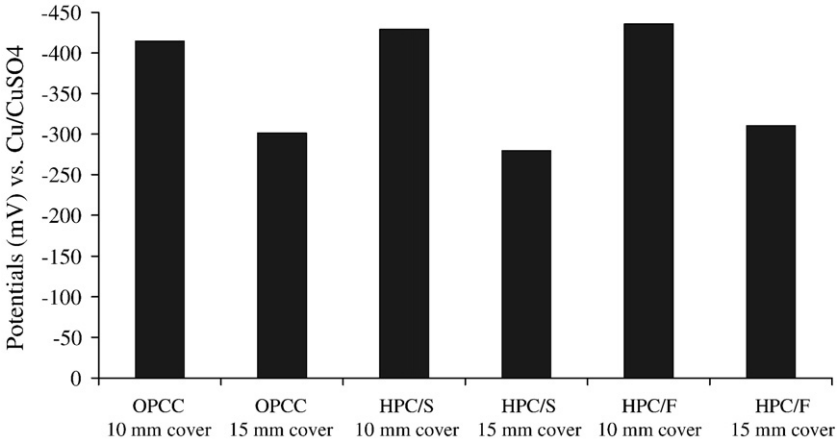

Fig. 9. Corrosion potential of the probes in prisms with 0.1 mm longitudinal crack, 128 weeks after exposure to de-icing salt.

ensure an induced crack intersected one of the probe elements. All probe elements and the stainless steel were electrically isolated from the main bar and from each other. After casting, the OPCC and HPC prisms were wet cured for 2 and 7 days, respectively. Then, the prisms were loaded in 4-point bending until a crack was formed. A stainless steel shim was inserted into the groove to retain the crack opening to 0.1 mm. Fig. 5 shows a schematic drawing of the prism. The prisms were covered with rock salt solution and kept wet and the corrosion activity of the steel probes was monitored using LPR measurements for over a 124 week period.

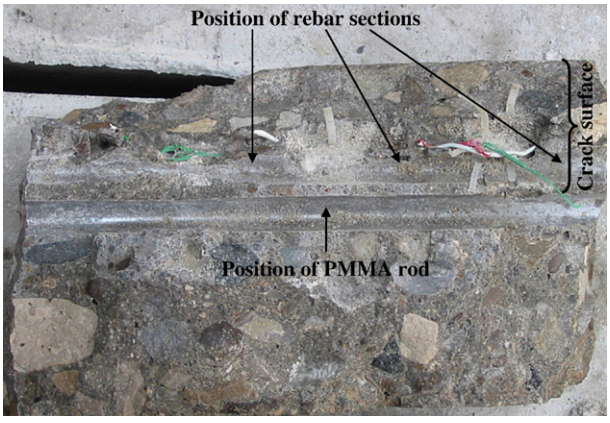

Fig. 10. Fracture surface of one of the prisms with 0.1 mm longitudinal crack, 128 weeks after exposure to de-icing salt.

2.3. Sound concrete specimens

A standard ASTM G109 specimen design [45] was used for determining the relative corrosion protection provided by the different concretes (without macrocracks) using both macrocell and microcell corrosion measurements. A comparison of the two measurements has been published [46]. The microcell data are used for comparison here. The specimen is illustrated schematically in Fig. 6 and the concretes were cast and cured as described above. The ponding well was filled with a 3 wt.% NaCl solution for two of every 4 weeks. Microcell corrosion was measured by using the LPR technique. For this purpose, the top bars were disconnected from the bottom bars for a period of 48 h to allow the system to stabilise. A saturated calomel electrode reference electrode and a stainless steel counter electrode were immersed in the ponding well as illustrated schematically in Fig. 7.

3. Results and discussion

The corrosion current densities of the top probes (10 mm cover) in specimens with 0.1 mm longitudinal crack, after 35 weeks of exposure to de-icing salt, are shown in Fig. 8. These data are the average of triplicate specimens and since the "percentage error"[1] (in this case, a measure of the variability) for all corrosion probes in the specimens for each type of concrete is less than 10%, presenting the average value is considered reasonable. In all cases, the steel is clearly in the passive

[1] Percentage error $= \left(\frac{\text{standard deviation}}{\text{mean value}}\right) \times 100$.

Fig. 11. Top steel probes recovered from three of the prisms with longitudinal crack after 128 weeks of exposure to de-icing salt: (a) before removing the corrosion products, (b) after removing the corrosion products.

state, with corrosion rates of ~4×10^{-4} A/m^2 or ~0.45 μm/year and there is no distinction between those embedded in OPCC and those in the HPCs. After 128 weeks exposure to salt, however, all the probe elements exhibited active corrosion. Corrosion current densities and corrosion potentials of the top probes (10 mm cover) and the lower probes (15 mm cover) are shown in Figs. 8 and 9, respectively. The average corrosion rates of the top probe elements are between 1.3×10^{-2} and 2.5×10^{-2} A/m^2 or 15–30 μm/year and their corrosion potentials all lie between −400 and −450 mV CSE. The probe elements with the 15 mm cover depth and, presumably, a lower chloride content, exhibit corrosion rates between 8×10^{-3} and 1.1×10^{-2} A/m^2 or 9–13 μm/year, with corrosion potentials between −280 and −300 mV SCE.

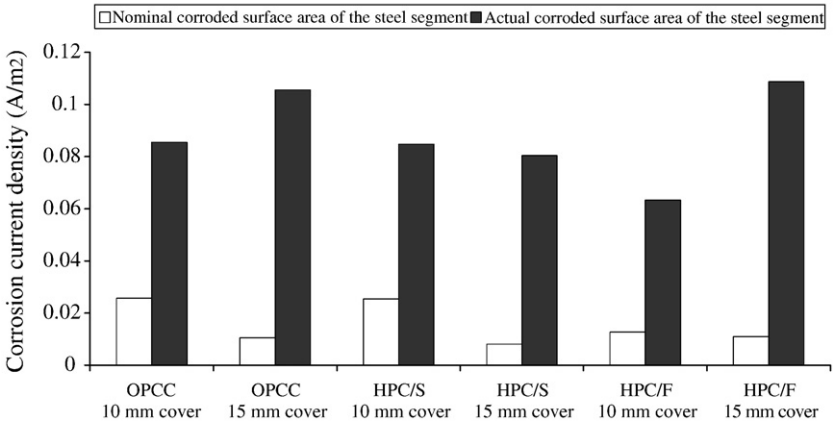

Fig. 12. Comparison between the corrosion current densities, calculated based on nominal and actual corroded surface areas.

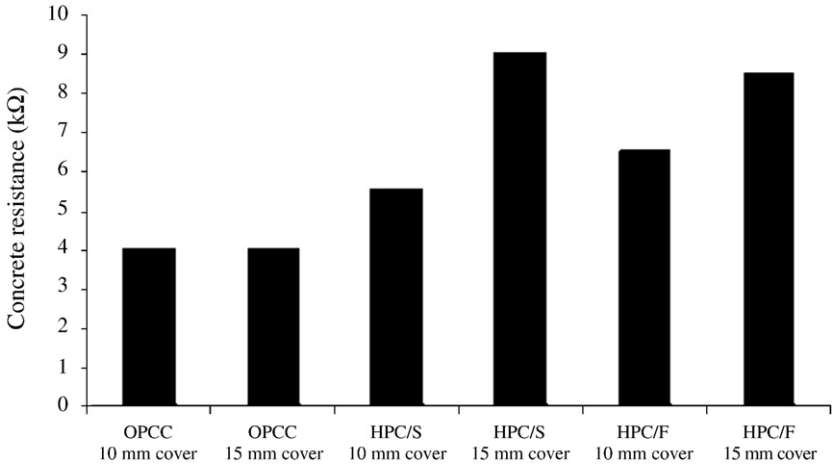

Fig. 13. Concrete resistance at different levels; prisms with 0.1 mm longitudinal crack; 128 weeks after exposure to de-icing salt.

Two observations can be made from these data: first that there is no significant difference between the corrosion rates and potentials of the steel in OPCC and those in HPC-slag (HPC/S) concretes. Second, the steel in top probes of the HPC-fly ash (HPC/F) concrete is corroding at a marginally lower rate but the steel with the greater cover depth exhibits the same rates as those in the other two concretes.

To confirm the results obtained by electrochemical measurements, prisms were broken and the steel probes and adjacent concrete were visually inspected. Visual observation of crack paths showed that they included the interface between the concrete and the steel rebars (Fig. 10). The bonding between concrete and the steel segments was also checked and showed that the segments were completely embedded in concrete (Fig. 11a) and the concrete compaction was good.

Results from visual observations are in agreement with corrosion measurements and verify that there is no apparent difference between the corrosion activities in OPCC and both HPCs. Continuous areas of the steel were covered with corrosion products as indicated in Fig. 11a. After removing the corrosion products, using an inhibited acid solution [47], the surface was clearly pitted as shown in Fig. 11b. However, the pits were distributed over an area of the surface, not specifically along the intersection with the crack because, as mentioned above, the crack continued around the surface of the steel. The actual corroded surface areas of the steel segments were estimated and the corrosion current densities were re-calculated based on these corroded areas and are given in Fig. 12 together with those based on the nominal areas. Although, the nominal corrosion current densities are higher at the top levels than the lower level, the actual corrosion rates at both levels are very close. It is concluded the chlorides reached the top bars first and initiated corrosion before reaching the lower bars. Thus, the top bars were corroding for a longer period during which the corroded area increased but the corrosion rate in the actively corroding locations is unchanged.

The resistances of the concretes, measured over a 70 mm diameter area encompassing the crack, after 128 weeks exposure, using galvanostatic pulse technique, are shown in Fig. 13. It is obvious that the resistances of both HPCs are significantly higher than that of OPCC, even at the crack. Therefore, considering the concrete resistance as an indicator for comparable corrosion activity, in HPC and OPCC may result in an under-estimation of the corrosion resistance provided by the HPC.

The corrosion rates of each probe in the prisms with the 0.1 mm transverse cracks after 124 weeks of exposure to salt solution are given in Fig. 14. It had been assumed that the crack would intersect one of the probe elements giving a higher corrosion rate for that probe element than for the other four. However, this was not the case: the highest corrosion rate occurred on different probe elements at different times. This could be attributed to a number of factors: (i) the crack intersecting two probes at their overlap point; (ii) crack branching and more than one crack at the level of the probes as has been observed in concurrent research [48]; (iii) and/or (iv) the effect of chloride diffusion from the crack surfaces. Consequently, the data in Fig. 13 are the average corrosion rates of the two probes with the highest corrosion rates in each of three replicate prisms.

In contrast to the corrosion behaviour of steel in the longitudinally cracked prisms, the corrosion current densities of steel in these HPCs are distinctly lower than those in the OPCC. Even after almost 2.5 years exposure in the laboratory to saturated salt solution, the corrosion current densities of both HPCs are in the passive range (10^{-3}–10^{-4} A/m^2 [40]) whereas steel in the OPCC has a similar corrosion rate to that of the steel in the longitudinally cracked HPC-slag with a 15 mm cover depth, i.e. ~0.007 A/m^2. Previous work [49,50] has shown that the corrosion of

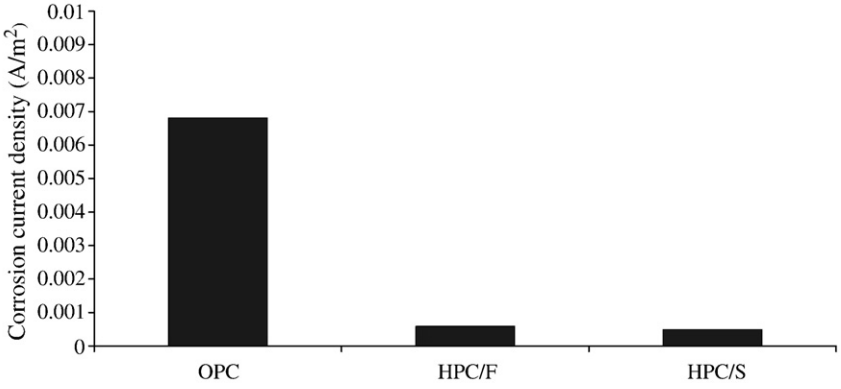

Fig. 14. Corrosion current density of the probes in prisms with 0.1 mm transverse crack, 124 weeks after exposure to de-icing salt.

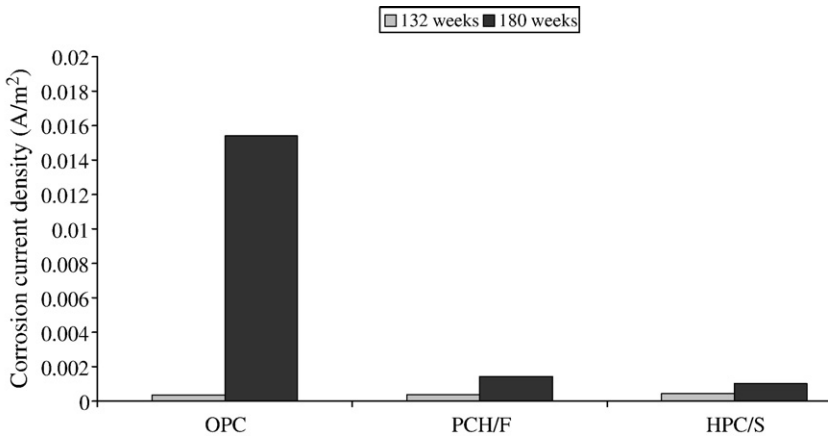

Fig. 15. Microcell corrosion current density of steel in sound concrete, 132 and 180 weeks after exposure to de-icing salt.

steel in HPCs is usually over a small area, probably confined to the tip of the crack, whereas the corrosion extends along the bar on either side of a crack in OPCC. However, in the current prisms, probably due to branching of the crack, this is not the case.

It should be mentioned that in the prisms with transverse cracks, the measured corrosion current density is lower than those of prisms with longitudinal crack. The reason is that the nominal surface area of the bars, not the actual corroding area, was used for the calculations. The corrosion at the tip of the crack in those samples was observed to be more localised.

The average values of microcell data from the steel in the sound concrete after 132 week of exposure are given in Fig. 15. As can be seen, there is no significant difference in corrosion rate of steel in the OPCC and both HPCs and the values all indicate passivity. Therefore, for comparative purposes, corrosion rates of these specimens after 180 days are also shown in Fig. 14. It is clear that, after this period, there is a very significant effect of concrete on the corrosion rates. The corrosion rates of the steel in the HPCs ($\sim 10^{-3}$ A/m^2) is at the upper end of the passive range, suggesting that there may be some active corrosion over a small area of the steel. On the other hand, the corrosion rate of steel in the OPCC was $\sim 1.6\times 10^{-2}$ A/m^2 and is clearly corroding.

4. Summary and conclusion

The behaviour of HPC containing 25% fly ash and HPC containing 25% slag is very similar in both sound and cracked concretes and so there is no apparent advantage to the use of one or the other.

There is no significant difference between resistance provided to rebar by OPCC and both HPCs when the concrete exhibits a longitudinal structural crack, even when the crack is only ~0.1 mm wide at the surface, i.e. well below the allowable limit of 0.3 mm given by the MTO.

When a 0.1 mm structural transverse crack exists, the HPC provides additional protection to the steel, by limiting the area of steel participating in the corrosion process for the anodic and cathodic half-cell components of the process. The protection is not as good as in sound concrete, but after about 124 weeks of exposure to de-icing salts, steel in both HPCs exhibits a corrosion rate at least five times lower than that of steel in OPCC.

High performance concrete, produced as specified by the MTO, provides vastly superior protection to steel in sound concrete than does a Class-C ordinary Portland cement concrete. For steel in both types of HPC, the corrosion rate is approximately an order of magnitude lower than that of steel in OPCC after 180 weeks exposure to chlorides.

The cover depth does influence the corrosion rate even when the bar is exposed to a longitudinal crack. However, the effect appears to be in the area of steel which is actively corroding: the corrosion current densities based on the nominal corrosion surface areas, are higher for probes with a 10 mm cover than for those with a 15 mm cover, but the actual current densities for the activity corroding areas are very similar. This indicates that increasing the chloride concentration, increases the corroded area but the local corrosion rate remains approximately constant.

For the longitudinally cracked concretes, the concrete resistances of both HPCs are higher than of OPCC while the corrosion current densities of steel in all concretes are very similar. Therefore, using concrete resistance as an indicator of corrosion in HPC is not recommended particularly at the locations of longitudinal cracks.

Acknowledgments

This research is part of a larger project on High Performance Concrete funded by the Cement Association of Canada (CAC), the Natural Sciences and Engineering Council of Canada and Materials and Manufacturing Ontario. The authors appreciate the support of Mr. Rico Fung of the CAC and gratefully acknowledge the assistance of Samuel Okulaja, Alain Laurent, Richard Morrison and Doug Hirst.

References

[1] ACI 318, Building Code Requirements for Structural Concrete, American Concrete Institute: Farmington Hills, MI, USA.
[2] P.P. Win, M. Watanabe, A. Machida, Penetration profile of chloride ion in cracked reinforced concrete, Cement and Concrete Research 34 (7) (2004) 1073–1079.
[3] MTO, SSP 904 S13 High Performance Concrete, Amendment to OPSS 904 Construction Specification for Concrete Structures. 1995, Ontario Provincial Standard Specification.
[4] S. Rostam, Reinforced concrete structures — shall concrete remain the dominating means of corrosion prevention? Materials and Corrosion 54 (6) (2003) 369–378.
[5] A.A. Ramezanianpour, V.M. Malhotra, Effect of curing on the compressive strength resistance to chloride — ion penetration and porosity of concretes incorporating slag, fly ash or silica fume, Cement & Concrete Composites 17 (1995) 125–133.
[6] Y. Ballim, Curing and the durability of OPC, fly ash and blast-furnace slag concretes, Materials and Structures/Materiaux et Constructions 26 (158) (1993) 238–244.
[7] N.R. El-Sakhawy, H.S. El-Dien, M.E. Ahmed, K.A. Bendary, Influence of curing on durability performance of concrete, Magazine of Concrete Research 51 (5) (1999) 309–318.
[8] R. Gagne, G. Henault, J. Marchand, In-situ and laboratory evaluation of chloride penetration and freeze–thaw durability of high performance concrete slabs, Proceedings of the Second International Conference on Concrete under Severe Conditions, E & FN Spon, Tromso, Norway, 1998.
[9] M. Pigeon, F. Garnier, R. Pleau, P.C. Aitcin, Influence of drying on the chloride ion permeability of HPC, Concrete International (1993) 65–69 (February).
[10] M.D.A. Thomas, C.M. Evans, Chloride penetration in high-performance concrete containing silica fume and fly ash, Proceedings of the Second International Conference on Concrete under Severe Conditions, E & FN Spon, Tromso, Norway, 1998.
[11] V. Baroghel-Bouny, P. Rogeau, T. Chaussadent, S. Care, Comparative study of the durability of ordinary and high performance concrete as part of the "BHP 2000" French National Project, International Symposium on High Performance and Reactive Powder Concretes, 1998, University of Sherbrooke, Sherbrooke, QC.
[12] P. Fidjestol, K. Tuutti, Chloride induced corrosion in high performance concrete — lifetime versus diffusivity and resistivity, Proceedings of the Second International Conference on Concrete under Severe Conditions, E & F N Spon, Tromso, Norway, 1998.
[13] N. Gowripalan, H.M. Mohame, Chloride-induced corrosion of galvanized and ordinary steel reinforcement in high-performance concrete, Cement and Concrete Research 28 (8) (1998) 1119–1131.

[14] J. Ryell, M.D.A. Thomas, P.R. Trunk, Properties of, and service life predictions for high performance concrete in transportation structures, Eight International Conference on Durability of Building Materials and Composites, 1999, NRC Research Press, Vancouver, BC.
[15] C. Hansson, S. Jaffer, and K. Olsen, Chloride threshold values for corrosion of steel in blended cement concretes. In press.
[16] P.K. Mehta, Concrete Structure, Properties and Materials, Prentice-Hall Inc., Englewood Cliffs, New Jersey, USA, 1986.
[17] M.E. Ismail, H.R. Soleymani, Monitoring corrosion rate for ordinary Portland concrete (OPC) and high performance concrete (HPC) specimens subject to chloride attack, Canadian Journal of Civil Engineering 29 (2002) 863–874.
[18] P.C. Aïtcin, A.M. Neville, P. Acker, Integrated view of shrinkage deformation, Concrete International, 1997, pp. 35–41.
[19] ACI committe 224, Causes, Evaluation and Repair of Cracks in Concrete Structures, American Concrete Institute, 1998.
[20] C. Andrade, C. Alonzo, F.J. Molina, Cover cracking as a function of rebar corrosion: Part II — numerical model, Materials and Structures 26 (1993) 532–548.
[21] R. Francois, G. Arliguie, A. Castel, Influence of service cracking on service life of reinforced concrete, Proceedings of the Second International Conference on Concrete under Severe Conditions, E & FN Spon, Tromso, Norway, 1998.
[22] A.W. Beeby, Cracking, cover and corrosion of reinforcement, Concrete International (1983) 35–40 (February).
[23] S. Moringa, Remaining service life of reinforced concrete structure after corrosion cracking, Durability of Building Materials and Components, E & F.N.Spon, Stockholm, Sweden, 1996.
[24] C. Andrade, C. Alonso, F.J. Molina, Cover cracking as a function of bar corrosion. Part I — experimental test, Materials and Structures 26 (1993) 453–464.
[25] R. Francois, G. Arliguie, Effect of microcracking and cracking on the development of corrosion in reinforced concrete members, Magazine of Concrete Research 51 (2) (1999) 143–150.
[26] R. Francois, G. Arliguie, Influence of service cracking on reinforcement steel corrosion, Journal of Materials in Civil Engineering 10 (1) (1998) 14–20.
[27] R. Weiermair, C.M. Hansson, P.T. Seabrook, M. Tullmin, Corrosion measurements on steel embedded in high performance concrete exposed to a marine environment, Third CANMET/ACI International Conference on Concrete in Marine Environment, American Concrete Institute, St. Andrews by the Sea, New Brunswick, Canada, 1996.
[28] A.R. Mendoza, Corrosion of reinforcing steel in loaded cracked concretes exposed to de-icing salts, Department of Mechanical Engineering, University of Waterloo, Waterloo, Ontario, 2003.
[29] C.M. Hansson, S.A. Okulaja, Corrosion of reinforcing steel in cracked high performance concrete, Advances in Cement and Concrete, University of Illinois at Urbana - Champaign, Copper Mountain, CO, USA, 2003.
[30] R. Weiermair, C.M. Hansson, P.T. Seabrook, M. Tullmin, The durability of high performance concrete in a marine environment, Concrete in Marine Environments, ACI, St. Andrews-by-the-Sea, 1995.
[31] T. Thuresson, C.M. Hansson, P.T. Seabrook, M. Tullmin, Effect of accelerated curing and cracking on the corrosion protection of steel embedded in high performance concrete, Durability of Concrete — Fourth CANMET/ACI International Conference, CANMET/ACI, Sydney, Australia, 1997.
[32] K. Okada, K. Kobayashi, T. Miyagawa, Influence of longitudinal cracking due to reinforcement corrosion on characteristics of reinforced concrete members, ACI Structural Journal 85 (2) (1988) 134–140.
[33] B. Shi, G. Zhao, Advance in bond behavior of concrete elements with corroded rebar, Jianzhu Cailiao Xuebao (Journal of Building Materials) 8 (6) (2005) 653–659.
[34] M. Maalej, S. Ahmed, P. Paramasivam, Corrosion durability and structural response of functionally-graded concrete beams, JCI International Workshop on Ductile Fiber Reinforced Cementitous Composites (DFRCC) — Application and Evaluation, 2002, Takayama, Japan.
[35] J.R. Roesler, J.S. Popovics, J.L. Ranchero, M. Mueller, D. Lippert, Longitudinal cracking distress on continuously reinforced concrete pavements in Illinois, Journal of Performance of Constructed Facilities 19 (4) (2005) 331–338.
[36] J.S. Miller, W.Y. Bellinger, Distress Identification Manual for the Long-term Pavement, Federal Highway Administration (FHWA), 2003.
[37] The facts about cracking in steel reinforced concrete pipe, Concrete Pipe Association of Australasia: http://www.concpipe.asn.au/Technical_Info/Publications_pdf/FactSheets/FS4_05.pdf.
[38] J.M. Ruiz, R.O. Rasmussen, G.K. Chang, J.C. Dick, P.K. Nelson, Computer-based guidelines for concrete pavements .Volume II — design and construction guidelines and HIPERPAV II user's manual, Office of Infrastructure Research and Development, Federal Highway Administration, 2005.
[39] Concrete pavement technology, in Early cracking of concrete pavement, causes and repairs 2002, American Pavement Concrete Association: http://www.iowaconcretepaving.org/ACPA%20Publications/tb016p.pdf.
[40] C.M. Hansson, Comments on electrochemical measurements of the rate of corrosion of steel in concrete, Cement and Concrete Research 14 (1984) 574–584.
[41] O.K. Gepraegs, C.M. Hansson, A comparative evaluation of three commercial instruments for field measurements of reinforcing steel corrosion rates, Electrochemical Techniques for Evaluating Corrosion Performance and Estimating Service-life of Reinforced Concrete, ASTM, West Conshohocken, PA, 2004.
[42] C.M. Hansson, P.T. Seabrook, T.D. Marcotte, In-place corrosion monitoring, Concrete International 26 (7) (2004) 59–65.
[43] MatWeb. 2006, http://www.matweb.com.
[44] C.M. Hansson, The effects of high performance concrete on corrosion of reinforcement, PCA R&D Project 00-07 Serial No. 2676, Portland Cement Association (PCA), 2004.
[45] ASTM G109-02, Standard Test Method for Determining the Effect of Chemical Admixtures on the Corrosion of Embedded Steel Reinforcement in Concrete Exposed to Chloride Environments, American Society for Testing Materials, West Conshocken, PA, 1992, pp. 451–455.
[46] C.M. Hansson, A. Poursaee, A. Laurent, Macrocell and microcell corrosion of steel in ordinary Portland cement and high performance concretes, Cement and Concrete Research 36 (2006) 2098–2102.
[47] ASTM, G1-90, Standard Practice for Preparing, Cleaning, and Evaluating Corrosion Test Specimens, ASTM, 1999.
[48] S.J. Jaffer, The Influence of Loading Mode and Concrete Type on the Corrosion of Steel in Concrete. PhD thesis in Mechanical Engineering, University of Waterloo, 2007.
[49] T.D. Marcotte, C.M. Hansson, The influence of silica fume on the corrosion resistance of steel in high performance concrete exposed to simulated sea water, Journal of Materials Science 38 (2003) 4765–4776.
[50] T.D. Marcotte, C.M. Hansson, A comparison of the chloride-induced corrosion products from steel-reinforced industrial standard versus high performance concrete exposed to simulated sea water, International Symposium on High Performance and Reactive Powder Concretes, University of Sherbrooke, Sherbrooke, Canada, 1998.